HHS Public Access

Inhibition, not excitation, drives rhythmic whisking

Martin Deschênes[1], **Jun Takatoh**[2], **Anastasia Kurnikova**[3], **Jeffrey D. Moore**[3], **Maxime Demers**[1], **Michael Elbaz**[1], **Takahiro Furuta**[4], **Fan Wang**[2], and **David Kleinfeld**[3,5]

[1]Department of Psychiatry and Neuroscience, Laval University, Québec City, Canada G1J 2R3

[2]Department of Neurobiology, Duke University Medical Center, Durham, NC 27710, USA

[3]Department of Physics, University of California, San Diego, La Jolla, CA 92093, USA

[4]Department of Morphological Brain Science, Graduate School of Medicine, Kyoto University, Kyoto 606-8501, Japan

[5]Section of Neurobiology, University of California, San Diego, La Jolla, CA 92093, USA

SUMMARY

Sniffing and whisking typify the exploratory behavior of rodents. These actions involve separate oscillators in the medulla, located respectively in the pre-Bötzinger complex (preBötC) and the vibrissa-related region of the intermediate reticular formation (vIRt). We examine how these oscillators synergize to control sniffing and whisking. We find that the vIRt contains glycinergic/ GABAergic cells that rhythmically inhibit vibrissa facial motoneurons. As a basis for the entrainment of whisking by breathing, but not vice versa, we provide evidence for unidirectional connections from the preBötC to the vIRt. The preBötC further contributes to the control of the mystacial pad. Lastly, we show that bilateral synchrony of whisking relies on the respiratory rhythm, consistent with commissural connections between preBötC cells. These data yield a putative circuit in which the preBötC acts as a master clock for the synchronization of vibrissa, pad and snout movements, as well as for the bilateral synchronization of whisking.

INTRODUCTION

Orofacial behaviors meet the need of basic physiological functions such as breathing, nutrient ingestion, active sensation, and social communication. Most of these activities involve periodic, rhythmic movements that must be coordinated in time and space. How nervous systems comply with biomechanical constraints and avoid antagonistic movements is a fundamental aspect of neurophysiology, and a model for coordinating neuronal computations that lead to motor acts. Here we address the issue of phase locking of rhythmic motor actions in the context of the synaptic mechanisms that coordinate whisking and

sniffing, which are predominant activities during exploratory behaviors in rodents (Deschênes and Kleinfeld, 2012; Kleinfeld et al., 2014).

Rats and mice rapidly and repetitively sweep their facial vibrissae back and forth to explore the environment. This activity, denoted whisking, is controlled by a neuronal oscillator located in the intermediate reticular formation (IRt) of the medulla, adjacent to the inspiratory oscillator for respiration, i.e., the pre-Bötzinger complex (preBötC; Moore et al., 2013; Feldman and Kam, 2015). This proximity is likely to be functionally relevant since whisking is tightly coupled to fast breathing, typically called sniffing. Yet even fast whisking is gated separately from breathing (Welker, 1964; Moore et al., 2013; Ranade et al., 2013). The vibrissa-related region of the IRt (vIRt) contains facial premotor neurons and neurons that fire either in phase or in antiphase with vibrissa protraction. Selective lesion of the vIRt abolishes whisking on the side of the lesion, and activation of the vIRt by iontophoretic injection of kainic acid (KA) induces long periods of continuous whisking in the lightly anesthetized rat (Moore et al., 2014). These results indicate that vIRt is both necessary and sufficient to generate the whisking rhythm. In both natural and KA-induced whisking intrinsic muscles that protract individual vibrissae follow the whisking oscillator, while extrinsic muscles that move the mystacial pad follow the breathing rhythm. The two rhythms are phase-locked on a cycle-by-cycle basis during rapid sniffing. The synaptic mechanisms for the control of different pools of facial motoneurons in a coordinated manner, as well as the synaptic mechanism for locking whisking with sniffing are not clearly established.

Here we examine how the vIRt and preBötC oscillators drive and phase-lock the activity of facial motoneurons during whisking. We first identified pools of motoneurons that control the facial muscles that move the mystacial pad versus the intrinsic muscles that drive only the vibrissae per se. Then we used virus injection, electrophysiological recordings during KA-induced whisking, and single cell labeling combined with in situ hybridization to determine how neurons in the vIRt and the preBötC phase lock the firing of specific pools of motoneurons. Finally, we validated results obtained under KA-induced whisking by recording the activity of facial motoneurons in alert head-restrained rats.

RESULTS

Facial muscles and their central representation

Anatomical background—Past studies have identified at least 18 different muscles that control the motion of rodent facial musculature, which includes the upper lip, the mystacial pad, the vibrissae, the nose and the nostril in rats and mice (Dorfl 1982; Haidarliu et al., 2010, 2012, 2015; Deschênes et al., 2015). Most of these muscles are recruited during exploratory behaviors, which involve the coordination of sniffing, whisking, nose and head movements (Welker, 1964). These muscles are anatomically mapped within the facial motor nuclear complex (Ashwell, 1982; Watson et al., 1982; Hinrichsen and Watson, 1984; Komiyama et al., 1984; Furutani et al., 2004; Klein and Rhoades, 1985; Takatoh et al., 2013; Sreenivasan et al., 2015). Motoneurons that innervate the intrinsic vibrissa muscles, for instance, are located in the lateral subnucleus, whereas those that innervate the nasolabialis muscle, responsible for retraction of the mystacial pad reside in the dorsal lateral subnucleus. However, the locations of the other motoneurons that translate the mystacial

pad, open the naris and deflect the nose remain uncharted. This information is critical to identify premotor circuits that coordinate motor commands to facial muscles and, in particular, to determine which facial muscles follow the motor commands associated with whisking as opposed to those associated with sniffing.

Retrograde labeling of facial motoneurons—The rostral part of the snout that lies in front of the mystacial pad is the site of origin of muscle nasolabialis profundus (Haidarliu et al, 2010). This muscle is comprised of several groups of fibers that attach to the nasal cartilage or to the premaxilla at the level of the incisors. These muscles slips are often collectively referred to as muscle nasalis following Dorfl (1982). Electromyographic and videographic recordings indicate that most, perhaps all of these muscles slips are active during the pre-inspiratory phase of the respiratory cycle, which is associated with the initial phase of vibrissa protraction (Hill et al., 2008; Moore et al., 2013; Deschênes et al., 2015). After placing a small pellet of Gelfoam saturated with DiI in the rostral part of the snout (3 rats), we observed retrogradely labeled neurons exclusively at the lateral most edge of the facial nucleus (Figure 1A).

Two extrinsic muscles, the nasolabialis and maxillolabialis, act in concert to retract the mystacial pad during whisking (Hill et al., 2008). Several studies have consistently located nasolabialis motoneurons in the dorsal lateral division of the facial nucleus (Watson et al., 1982; Komiyama et al., 1984; Takatoh et al., 2013; Sreenivasan et al., 2015). To identify the pool of motoneurons that innervate the maxillolabialis muscle, which pulls the mystacial pad in the ventrocaudal direction, we first dissected facial tissue behind the gamma and delta vibrissae. We then used microstimulation to identify the maxillolabialis muscle, based on ventrocaudal vibrissa deflections concurrent with stimulation. Fluorogold injection into muscle maxillolabialis (3 rats) produced retrograde labeling in the dorsal part of the facial nucleus, medial to motoneurons that innervate muscle nasolabialis (Figure 1B).

We further mapped the location of motoneurons that control motion of the nose. Muscle deflector nasi, which was previously known as muscle naris dilator (Deschênes et al., 2015), was also identified by microstimulation and injected with Fluorogold (3 rats). As for the case of the vibrissa retractor muscles, we observed retrogradely labeled motoneurons in the dorsal lateral sector of the facial nucleus (Figure 1C).

Transsynaptic labeling of premotor neurons—Prior transsynaptic labeling studies have identified several pools of premotor neurons that control the intrinsic vibrissa muscles and the nasolabialis muscle (Takatoh et al., 2013; Sreenivasan et al., 2015). Here we extend these studies to the snout. We injected ΔG-Rabies-mCherry in the tip of the snout to label premotor neurons that control muscle nasolabialis profundus (3 juvenile mice). As in the cases where DiI was injected in the rostral part of the snout, retrogradely labeled motoneurons are found at the lateral most edge of the facial nucleus (Figure 1D). The vast majority of transsynaptically labeled premotor neurons are found in the ipsilateral preBötC, with some cells scattered in the ipsilateral parafacial and caudal parvocellular reticular formation. A small fraction of cells are also labeled in the contralateral preBötC. No transsynaptic labeling is present in the trigeminal sensory nuclei, nor in rostral mesencephalic regions – i.e., the Kölliker-Fuse nucleus, red nucleus, and superior colliculus.

As a control, G-Rabies-mCherry was injected into the mystacial pad to label premotor neurons that control the intrinsic vibrissa muscles (Figure 1E). These injections produce conspicuous transsynaptic labeling in the ipsilateral vIRt, as well as in the other brainstem regions as reported previously (Takatoh et al., 2013; Sreenivasan et al., 2015). Together, the results from transsynaptic labeling suggest that neurons in the vIRt and the preBötC directly innervate different groups of facial muscles.

Summary of both prior anatomical data and the above mapping results define a myotopic map of the facial motor nucleus (Figure 1F). It shows a musculotopic organization of the snout, with the extrinsic vibrissa muscles represented laterally and dorsolaterally, and the intrinsic muscles represented in the ventral lateral part of the facial nucleus.

Projections of preBötC and vIRt cells to the facial nucleus

On the basis of retrograde labeling and of the size of focal lesions that abolish whisking, facial-projecting cells in the vIRt form a narrow column that is located medially to the preBötC (Moore et al., 2013). This column spans about 400 μm rostrocaudally, 200 μm mediolaterally, and 400 μm dorsoventrally. We sought to verify the projection patterns of the vIRt and preBötC premotor regions via complementary anterograde tracing. Since neurons in both the vIRt and the preBötC project to the facial nucleus, this mapping requires precise anterograde tracer injections that do not straddle these two nearby regions. We first located the preBötC electrophysiologically, and injected small volume of Sindbis-GFP virus in the lateral portion of the preBötC (Figure 2A) or in the medial portion of vIRt (Figure 2E) to maximize the separation of the injection sites (3 rats; see also Figure S1). This approach reveals complementary projection patterns in the facial nucleus. Neurons from the preBötC project preferentially in a crescent-shaped region at the lateral and dorsal lateral border of the nucleus (Figures 2C and 2D), while neurons from the vIRt project principally to the ventral lateral region, just medially to the preBötC terminal zone (Figures 2F and 2G). Sindbis-GFP injections in the preBötC, but not in vIRt, also produce terminal labeling contralaterally in the lateral part of the facial nucleus. In contrast, virus injections in the inspiratory bulbospinal ventral respiratory group (3 rats) do not produce terminal labeling in the facial nucleus.

We further determined the neurotransmitter content of preBötC cells that project to the facial nucleus by combining retrograde labeling with in situ hybridization (Figure 2H and 2I). We found that $68 \pm 10\%$ (mean ± SD; 79 cells in 3 rats) of the retrogradely labeled preBötC cells express the vGluT2 (vesicular glutamate transporter type 2) transcript, while $23 \pm 3\%$ (16 out of 70 cells in 3 rats) express the VGAT (vesicular GABA transporter) transcript. These results indicate that input to the facial nucleus from the preBötC is mainly glutamatergic, and that it targets principally motoneurons that innervate the extrinsic muscles. In contrast, afferents from the vIRt terminate principally in a more medial region of the lateral facial nucleus that contains motoneurons that innervate the intrinsic vibrissa muscles.

Firing of facial motoneurons during KA-induced whisking

Facial motoneurons have extensive dendritic trees that spread across the subnuclear domains defined by their target region (Friauf, 1986; Nguyen et al., 2004; Herfst and Brecht, 2008). To assess the selectivity of activation by the whisking and respiratory central rhythm generators (CRGs), we recorded rhythmic activity of 128 facial motoneurons during KA-induced whisking in 8 rats lightly anesthetized with ketamine-xylazine. This preparation was used to decouple whisking and breathing, and determine which motoneurons relate to each of the rhythms (Moore et al., 2014). We observed that 66% of these neurons discharged spike bursts phase-locked with vibrissa protraction – we designated these cells as whisking motoneurons. The remaining neurons fired during either the inspiratory (24%) or the expiratory phase (10%) of the breathing cycle – we designate these cells as respiration-modulated motoneurons. Critically, no motoneuron fired in phase with retraction of the vibrissae, and none of the motoneurons displayed both whisking and respiratory modulation. Finally, labeling either single cells or the recording sites with Neurobiotin confirmed that respiratory motoneurons are located in the dorsal lateral and lateral most sectors of the nucleus, while whisking motoneurons are located more ventrally in the lateral region (Figure S2).

Intracellular recording of whisking motoneurons (15 neurons) revealed sawtooth-like membrane potential oscillations characterized by a slow ramping, jaggy depolarization crowned with action potentials during vibrissa protraction, along with a sharp repolarization at the onset of retraction (Figures 3A–C). Membrane hyperpolarization to approximately −70 mV, the equilibrium potential of Cl^- in facial motoneurons (Toyoda et al., 2003), markedly reduced the amplitude of subthreshold oscillations (Figure 3D). This suggests that periodic perisomatic inhibitory postsynaptic potentials (IPSPs) constitute a dominant component of the oscillatory behavior. We confirmed the inhibitory nature of the input via intracellular injection of chloride (3 cells), which reverses the polarity of IPSPs, and inverts the phase of the intracellular oscillations (Figures 3E and 3F). From these results, we infer that the slow depolarizing ramp consists of excitatory events that occur in the dendrites, whereas the fast repolarization is mediated by perisomatic IPSPs.

In contrast to the case of vibrissa motoneurons, the amplitude of subthreshold oscillations in respiration-modulated motoneurons increases upon membrane hyperpolarization (8 cells; Figures 3G and 3H). At a typical resting potential of −60 to −55 mV, we saw no indication of hyperpolarizing postsynaptic potentials associated with breathing. In four of these cells, with at least 10 minutes of recording time, Cl^- injection did not change the phase of membrane potential oscillations with respect to that of the respiratory rhythm. Thence, rhythmic excitatory postsynaptic potentials (EPSPs) appear to drive membrane potential oscillations in motoneurons modulated by respiration. On the basis of these data, one can conclude that despite the extensive overlap of dendritic fields in the facial nucleus, afferents from the vIRt and preBötC exert a selective drive on whisking and respiration-modulated motoneurons, respectively.

Neurotransmitter phenotype and phase locking of vIRt cells

Prior recordings of vIRt cells during KA-induced whisking revealed two populations of neurons with antiphasic firing patterns (Moore et al., 2013) - i.e., units that fire during vibrissa protraction (27%), and units that fire during vibrissa retraction (73%). In light of the inhibitory rhythmic oscillations recorded in whisking motoneurons, we asked whether vIRt cells that discharge during protraction or retraction are glutamatergic or glycinergic/GABAergic. We assessed the phase relationship of vIRt cells (93 cells in 17 rats) that displayed rhythmic bursts during KA-induced whisking, juxtacellularly labeled a subset of these cells with Neurobiotin, and used in situ hybridization to determine whether labeled cells express the VGluT2 or the VGAT transcript.

Recordings were carried out under one of two conditions. One set made use of light ketamine/xylazine anesthesia (66 cells in 11 rats). Here all cells displayed phase-locked firing patterns (Figures 4A and 4B) either for protraction (30%) or retraction (70%) with a high degree of spectral coherence between spiking activity and vibrissa motion at the peak frequency of whisking (ICoherenceI = 0.94 ± 0.03 and 0.90 ± 0.09 for protraction and retraction units, respectively). Ten vIRt cells were labeled jusxtacellularly, one per animal, and processed for in situ hybridization. All retraction units (5 cells) expressed VGAT (Figure 4C), but only one out of five protraction units expressed the VGluT2 transcript (Figure 4D). This indicates that a majority of vIRt cells that discharge rhythmically during vibrissa protraction are not glutamatergic.

A second set of recording made use of rats initially anesthetized with urethane (700 mg/kg) supplemented with a one-third dose of ketamine/xylazine (27 cells in 6 rats). This anesthetic regimen was used to prolong the whisking period during which vIRt cells could be stably recorded. Unexpectedly, all rhythmic vIRt cells recorded under urethane anesthesia were retraction units (purple circles in Figure 4B), with neighboring units that discharged in a sustained manner. Mean coherence between rhythmic spike bursts and whisk cycle at the whisking frequency (IcoherenceI = 0.93 ± 0.07) was not significantly different from that of retraction units recorded under ketamine anesthesia (two-sample t-test; p= 0.65). Together, the electrophysiological and in situ data imply that rhythmic bursting of protraction units is not required for KA-induced whisking in urethane-anesthetized rats. Rather, inhibitory vIRt cells that discharge in phase with vibrissa retraction appear sufficient to generate whisking.

Firing patterns of facial motoneurons during natural whisking

Although KA-induced whisks display a frequency range and kinematics similar to self-generated whisks in alert rats (Moore et al., 2014), one may ask whether the firing pattern of facial motoneurons during KA-induced whisking is consistent with that observed during natural whisking. Of central interest, we sought to determine if self-generated whisking involves rhythmic inhibition of motoneurons that drive the intrinsic vibrissa muscles. We thus recorded from facial motoneurons in alert head-restrained rats. Single unit recordings from calm but whisking animals revealed two populations of rhythmic cells: motoneurons that fire during protraction of the vibrissae (24 cells in 3 rats), and motoneurons that fire during respiration or sniffing (15 cells in 3 rats). The former motoneurons were distinguished from respiration-modulated motoneurons by their rhythmic discharges during

intervening whisks, which are whisks that are not associated with a breath (Moore et al., 2013; Figure 4D). As in the KA model of whisking, no motoneuron fired preferentially during vibrissa retraction, and none of the motoneurons displayed both whisking and respiratory modulation.

Whisking motoneurons—Motoneurons active during low-amplitude whisks increased their firing rate with the amplitude of vibrissa protraction, and additional motoneurons were recruited as the amplitude of vibrissa movement increased (Figure 4D). Retraction of the vibrissae was associated with an arrest of discharges but, given the low discharge rates before whisking bouts, it was unclear whether the arrest of discharges was caused by rhythmic inhibition. To address this issue, we needed to record from aroused animals with sustained bouts of high amplitude whisking. The associated motion precluded the use of unit recording from facial motoneurons, so we turned to electromyogram (EMG) recording of intrinsic motor units (3 rats). These data reveal that whisking bouts occur on a background of sustained discharges (81 ± 21 Hz, mean $\pm$ SD; range: $47 - 124$ Hz) when the vibrissae are maintained in a protracted position (Figure 4F). We selected 15 sequences containing both basal respiration and sniffing bouts during which two to three motor units could be discriminated. We assessed the firing rates as a function of phase in the breathing cycle during basal respiration (frequency < 4 Hz) and during sniffing associated with whisking (frequency > 4 Hz). Circular histograms of Figures 4G and 4H show that during basal respiration, in the absence of whisking, motor units fire during both the inspiratory and expiratory phases of the breathing cycle, with 45% of spikes occurring during expiration. In contrast, during sniffing associated with whisking, the fraction of spikes emitted during expiration (or vibrissa retraction) drops to 21%, which is significantly smaller than the fraction of spikes emitted during basal respiration (z-test, $p < 0.0001$). Given that vibrissa retraction and expiration are tightly phase-locked, these data strengthen the argument that inhibitory drive on intrinsic motoneurons is the key mechanism in whisking generation.

Respiration-related motoneurons—Among respiration-related motoneurons, some fired in a one-to-one manner with each inspiration during both basal respiration and sniffing (4 cells in 3 rats), while others were mainly recruited during high respiratory drive (11 cells in 3 rats; Figures 5A and 5B). In both cases rhythmic firing was locked to either the inspiratory or the expiratory phase of breathing (Figure 5C). We carried out EMG recordings from muscle nasolabialis to further specify the identity of muscles active during basal respiration versus sniffing. These recordings reveal motor units that are preferentially active during the expiratory phase of sniffing versus basal respiration (Figures 5E and 5F). As reported previously (Moore et al., 2013), nasolabialis activity is absent during intervening whisks, and shifts from late expiratory during basal respiration to early expiratory during sniffing. Given their small size, the EMG from the different slips of muscle nasolabialis profundus cannot be recorded individually. Nonetheless two types of motor units were found. The first was active during inspiration at all breathing frequencies, while the second was principally active during inspiration when the animal sniffs (Figures 5G and 5H). In summary, our EMG recordings recapitulate the firing patterns of facial motoneurons, and independently confirm that nasolabialis motoneurons and some motoneurons that innervate muscle nasolabialis profundus are preferentially recruited during sniffing.

Unidirectional connections between the preBötC and vIRt

Phase sensitivity analysis of coupling between whisking and breathing has shown that inspiration can reset whisking, but not vice-versa (Moore et al., 2013). From an anatomical perspective, this could be implemented via unidirectional connections from the preBötC to the vIRt. We made small injections of Sindbis-GFP virus into the preBötC (3 rats), and indeed found a large number of GFP-positive terminals in the vIRt (Figures 6A and 6B; see also Figure S3). In contrast, small Sindbis-GFP injections into the vIRt (3 rats) resulted in dense anterograde labeling in the ventral lateral region of the facial nucleus, but no significant anterograde labeling in the preBötC (Figures 6C and 6D; see also Figure S3). These results lend strong support to the notion that phase resetting of whisking by basal respiration and sniffing is mediated by unidirectional connections from the preBötC to the vIRt.

Bilateral whisking is synchronized by the respiratory CRGs

In the absence of external objects or head turning, natural whisking is bilaterally synchronous (Gao et al., 2003; Sachdev et al., 2003; Towal and Hartmann, 2006; Mitchinson et al., 2007), which requires a circuitry that coordinates the activity of the left and right whisking CRGs. Yet, bilateral injections of KA result in incommensurate vibrissa motion (Moore et al., 2014), as measured in anesthetized animals, suggesting a lack of direct coupling between the left and right vIRts (Figures 7A and 7B). We assessed the independence of vIRt oscillators in alert rats by comparing the degree of bilateral coherence between sniff-locked and intervening whisks (Figure 7C). If both oscillators are independent from one another, one expects intervening whisks to drift in phase when the respiratory CRG is transiently halted. We therefore selected whisking bouts that occurred after spontaneous sighs, when the expiratory period lasted for at least 500 ms, and compared them with random segments of whisking while sniffing. Spectral analysis reveals a significant diminution of coherence for intervening whisks, together with high variability (Figure 7D) and a phase shift (Figure 7E), which is consistent with the notion that the two whisking CRGs are independent from one another, and therefore begin to drift in the absence of repeated resetting events. Lastly, we injected Neurobiotin into the vIRt during KA-induced whisking, and compared the amount of anterograde labeling in the contralateral vIRt with that in the lateral facial nucleus (2 rats). While numerous boutons were found in the lateral facial nucleus, the contralateral vIRt was nearly devoid of terminal labeling (Figure S4). These data are consistent with the lack of vIRt-to-vIRt commissural connections.

DISCUSSION

The putative brainstem circuitry that generates and coordinates whisking is summarized in Figures 8A and 8B. The core of the whisking CRG consists of glycinergic/GABAergic vIRt cells that inhibit facial motoneurons that control the intrinsic vibrissa muscles, thus causing synchronous retraction of the ipsilateral vibrissae. The persistence of KA-induced whisking in absence of protraction units in the vIRt dismisses the possibility that the whisking rhythm relies on a push-pull mechanism that involves reciprocal connections between protraction and retraction units. Rather, the core of the whisking CRG likely consists of interconnected inhibitory vIRt cells, i.e., retraction units that are endowed with intrinsic oscillatory

properties. The role of the small population of glutamatergic vIRt cells that project to the facial nucleus remains unknown; one possibility is that it contributes to driving vibrissa protraction and enhancing whisk amplitude, together with other excitatory (modulatory) inputs that contact motoneurons innervating the intrinsic vibrissa muscles.

Motoneurons that control the extrinsic muscle groups are driven by the respiratory network, which includes premotor neurons in the preBötC and putative follower cells that are located in the parafacial region (Pagliardini et al., 2011). The target of inhibitory preBötC cells that project to the facial nucleus is unknown. This projection could drive antagonistic muscles that control opening and closing of the nares, or again the activity of narial muscles that move the upper lip and the tip of the nose. The resetting of whisking by the respiratory CRG is mediated by axonal projections from the preBötC to the ipsilateral whisking CRG, while bilateral whisking synchronization relies on commissural connections between the two preBötCs.

Bilateral synchronization of whisking is mediated by the respiratory CRG

The lack of vIRt-to-vIRt connections is in line with the absence of synchronous whisking after bilateral injection of KA, and with the phase drift of intervening whisks when respiration is transiently suppressed during a sigh. Together these results indicate that commissural connections between vIRTs are either absent or, if present, they are not strong enough to synchronize whisking bilaterally. Alternatively, several studies have clearly established that glutamatergic preBötC cells are interconnected by commissural axons (Wang et al., 2001; Stornetta et al., 2003; Koizumi et al., 2013). Impairment of these connections in Robo knock-out mice leads to desynchronization of the excitatory drive to the left and right spinal and cranial motoneurons (Bouvier et al., 2010). In light of the fact that each preBötC projects to vIRt, commissural connections between the respiratory pattern generators represent a likely substrate for the bilateral synchronization of whisking, which is conditional on respiratory phase-resetting.

Beyond the intrinsic/extrinsic muscles dichotomy

Neuronal mechanisms that generate whisking are usually discussed in terms of coordinated activation of the intrinsic and extrinsic muscle groups. However, this dichotomy does not account for the actual diversity of facial muscles that are active during sniffing and whisking. As a case in point, muscle nasolabialis profundus, usually referred to as muscle nasalis, has two major components: one that attaches to the plate of the mystacial pad (pars *maxillaris*), which contributes to dilation of the nares (Deschênes et al., 2015), and another one that attaches to the corium (*pars media*), which translates the mystacial pad rostrally (Hill et al., 2008; Haidarliu et al., 2012, 2015). Both muscle components contract at the onset of inspiration. While naris dilation occurs with each inspiration in awaked rats, rostral translation of the pad occurs primarily when the rate or amplitude of respiration increase, irrespective of whether the animal whisks (Hill et al., 2008; Deschênes et al., 2015). The same is true for the extrinsic retractor muscles (nasolabialis and maxillolabialis) and the nasi deflector muscle, which are principally active when the animal sniffs or whisks (Figures 5F–H) (Sherrey and Megirian, 1977; Deschênes et al., 2015. The recruitment of these muscles during sniffing likely depends on modulatory action that enhances the excitability of the

motoneurons themselves or of the associated premotor circuits. Figure 8C illustrates the time-ordered patterns of neuronal and muscular activities associated with the different phases of the respiratory and whisking rhythms for sniffing as well as basal respiration.

Conditional respiratory drive to facial motoneurons

While our results provide clear evidence for the key role of inhibitory vIRt cells in whisking generation, premotor circuits that activate motoneurons that drive the extrinsic muscle groups remain less well delineated. Activation of latter muscles is tightly coupled to the respiratory cycle (Moore et al., 2013), which is consistent with the strong respiratory drive in motoneurons of the dorsal and lateral facial subnuclei, and with the bilateral projection of the preBötC to the same subnuclei. By and large, preBötC cells that constitute the respiratory pattern generator are glutamatergic and express somatostatin or the neurokinin-1 receptor. Interestingly, Takatoh et al. (2013) reported that few preBötC cells labeled after G-rabies injection in the mystacial pad express these phenotypes. Furthermore, injection of an adeno-associated virus that expresses eGFP driven by the somatostatin promoter in the preBötC did not label terminal fields in the facial nucleus (Tan et al., 2010). Since the deletion or silencing of neurokinin-1 receptor and somatostatin-expressing preBötC neurons, respectively, disrupts breathing in the adult rat (Gray et al., 2001; Tan et al., 2008), the preBötC projection to facial motoneurons may arise from cells that are not themselves part of the respiratory CRG. The latter cells may be recruited when the animal sniffs, or the conditional respiratory drive may involve follower neurons intercalated between the preBötC and facial motoneurons. The region immediately caudal to the facial nucleus appears as a potential source of this conditional drive. It contains facial premotor neurons (Moore et al., 2013), and exploratory recordings in this region revealed a number of neurons that are recruited during acceleration of the breathing rhythm (unpublished data). However, it remains unclear whether these cells are part of the parafacial respiratory group as delineated in prior studies (Fortuna et al., 2008; Abbott et al., 2011; Pagliardini et al., 2011).

Innervation of the lateral most sector of the facial nucleus by preBötC neurons is consistent with the phasic activation of nasolabialis profundus motoneurons during inspiration. Sindbis injection in the preBötC also led to anterograde labeling in the dorsal lateral region of the facial nucleus where expiratory motoneurons that drive the extrinsic retractor muscles are clustered. This result is consistent with the retrograde labeling of premotor neurons in the preBötC after G-rabies injection in muscle nasolabialis in mice (Takatoh et al., 2013; Sreenivasan et al., 2015). Intracellular recordings revealed that motoneurons in the dorsal lateral facial subnucleus receive excitatory input phase locked to expiration. It should be pointed out that although the vast majority of cells in the preBötC are active during inspiration, expiratory neurons are also commonly recorded in this medullary region (Shao and Feldman, 1997; Guyenet and Wang, 2001). Therefore, motoneurons that innervate the extrinsic retractor muscles may receive direct excitatory input from expiratory preBötC cells that are recruited during sniffing.

Conclusion

The behavior of rodents is dominated by rhythmic orofacial activities, i.e., whisking, breathing, sniffing, suckling, licking, swallowing, ultrasonic calls (Welker, 1964; Sirotin et

al., 2014; Kleinfeld et al., 2014), that involve the coordinated recruitment of facial muscles, tongue muscles and several muscle groups of the upper airways. Coordination of these activities requires a hierarchal organization of the brainstem circuitry so that their occurrence and timing do not interfere with fundamental metabolic needs. From this standpoint, respiration is more than a rhythm for life, but it also coordinates orofacial motor commands that engage common muscle groups and serve a variety of active sensory, ingestive, and social behaviors.

EXPERIMENTAL PROCEDURES

Experiments were carried out in 84 Long Evans rats (250–350 g), four Wistar rats (250–350 g), and six Chat: :Cre; RΦGT juvenile mice [19] (P10 at end point) according to the National Institutes of Health Guidelines. All experiments were approved by the Institutional Animal Care and Use Committee at Laval University, the University of California of San Diego, Duke University, and University of Kyoto.

Electrophysiology in anesthetized rats

Most experiments were carried out under ketamine (75 mg/kg)/xylazine (5 mg/kg) anesthesia. A few experiments (6 animals) were also carried out under light urethane anesthesia (700 mg/kg) supplemented with one-third the above dose of ketamine/xylazine. Body temperature was maintained at 37.5°C with a thermostatically controlled heating pad. Respiration was monitored with a piezoelectric film (cantilever type; LDT1 028K; Measurement Specialities) resting on the rat's abdomen just caudal to the torso. All vibrissae, but one of C2 or D2, were cut near the skin, and vibrissa motion was monitored with a Basler A602f camera operated in line-scan mode with a 1-kHz scan rate at a spatial resolution of 120 μm per pixel. Motion was imaged along a line that was 5 to 10 mm from the edge of the mystacial pad. Pixel intensity along the line was thresholded, and the centroid of the detected vibrissa was converted to a voltage proportional to pixel position in real time.

Extracellular and juxtacellular recordings were carried out with micropipettes (tip diameter, 1 μm) filled with 0.5 M potassium acetate plus 2% (w/v) Neurobiotin (Vector Labs). Intracellular recordings were performed with similar micropipettes filled with either 0.5 M potassium acetate, or 2 M potassium chloride. Intracellular chloride injection was carried out by passing negative DC current (2–5 nA) for 5 to 8 min. Recording sites or individual cells were labeled extracellularly or juxtacellularly according to the method described by Pinault (1996). All signals were sampled at 10 kHz and logged on a computer using the Labchart acquisition system (AD Instruments).

Electrophysiology in alert head-restrained rats

Rats were habituated to body restraint for 5 days. Then they were implanted with a custom-built head-restraining mount, and a thermocouple (K-type; Omega Engineering) was placed in the nasal cavity to monitor respiration (Moore et al., 2013). Surgical procedures were carried out in animals anesthetized with ketamine (75 mg/kg) and xylazine (5 mg/kg). Rats were allowed to recover for 3 days before the onset of behavioral experiments. During the

recording sessions, rats were placed inside a body-restraining cloth sack and rigid tube, and the animals were head-restrained. Rats were briefly anesthetized with isoflurane, and a craniotomy was performed over the cerebellum to get access to the facial nucleus. A drop of local anesthetics (bupivacaine) was applied over the dura, and the dura was open by local heating with a fine-tip cauterizer. Anesthesia was stopped, and neuronal activity was recorded in the facial nucleus using quartz micropipettes with a tip diameter of 4–8 μm, filled with 2% (w/v) Chicago sky blue (Sigma) in 0.5 M NaCl. All vibrissae except C2 or D2 were cut at the base, and movement of the intact vibrissa was monitored on line with a Basler A602f camera operated in line-scan mode. Rats were coaxed to whisk by presenting food or bedding from the home cage (Ganguly and Kleinfeld, 2004). One recording site was marked in each rat with an iontophoretic deposit of Chicago sky blue (5–10 μA with 10-s pulses spaced every 20 s for 5 min). Rats were deeply anaesthetized at the end of the session and perfused with phosphate buffered saline (PBS), and then with 4% (w/v) paraformaldehyde in PBS. Brains were post-fixed for 2 h, cryoprotected in 30% (w/v) sucrose in PBS, and sectioned along the coronal plane at a thickness of 50 μm with a freezing microtome. Sections were stained for cytochrome oxidase. Data were obtained from 3 rats in which the deposit of Chicago sky blue was found in the lateral part of the facial nucleus.

In a separate series of experiments, five rats were head restrained, and two pairs of teflon-coated tungsten wires, each 50 μm in diameter, were inserted in facial muscles under isoflurane anesthesia. Using a 25G hypodermic needle, hooked wires were placed in the mystacial pad, in nasolabialis muscle, or in the rostral part of the snout to record the activity of the nasolabialis profundus muscles. Connecting leads were mechanically floated to exert minimal drag on the tissue, and increase the likelihood of obtaining stable recording of single motor units. Electromyographic activity was recorded differentially, bandwidth: 200 Hz – 5 kHz, and vibrissa movement was monitored as described.

Kainic acid injection

Full description of the KA protocol for inducing whisking in anesthetized rats has been published (Moore et al., 2014). Briefly, micropipettes with 8 – 10 μm diameter tips were filled with kainic acid, 1% w/v in 0.1 M Tris buffer, pH 8.3, and lowered in the brainstem at the following stereotaxic coordinates: frontal plane, 12.6 mm behind the bregma; lateral plane, 1.5 mm from the midline; depth, 7.4 mm below the pial surface. Kainic acid was delivered by iontophoresis with –400 nA, 1 s duration current pulses delivered at 50% duty cycle for 10 min.

Retrograde and anterograde labeling

For details on tract tracing see supplemental experimental procedures.

Data analysis

The relationship between unit activities and the whisking or breathing rhythms was estimated by computing the spectral coherence (Mitra and Pesaran, 1999). Single whisks or breaths were isolated by band-pass filtering the position traces between 1Hz and 25Hz with a 3-pole Butterworth filter run in forwards and backwards directions, and applying the

Hilbert transform (Hill et al., 2008). The Chronux toolbox (http://www.chronux.org) was used to compute coherence between spike times or intracellular events averaged over 2-s segments with a time-bandwidth product of two. Basal respiration was defined as the instantaneous respiratory frequency below 4 Hz, and sniffing as the instantaneous respiratory frequency greater than 4 Hz. We report the magnitude and phase of the coherence at the peak frequency of whisking or breathing. A phase of zero corresponds to the peak of protraction or inspiration.

The degree of bilateral coherence between sniff-locked and intervening whisks was analyzed in 3 head-restrained rats. We selected intervening whisks occurring after a sigh, when respiration is transiently halted. This analysis was performed with 15, 40, and 38 intervening whisk clips, and 128, 23, and 73 clips of whisking while sniffing, in each of the three rats respectively. In total, this corresponds to 17.4 s of intervening whisks and 238.4 s of sniffing in rat #1, to 26.5 s of intervening whisks and 50.9 s sniffing in rat #2, and 34.1 s of intervening whisks and 107.3 s of sniffing in rat #3.

Analysis of motor unit activity was carried out using spike sorting (Labchart 7.3) and custom-written scripts in Matlab. We chose sequences that contained both basal respiration and sniffing bouts associated with whisking, and during which motor units discharges in a sustained manner. Circular phase histograms of motor unit discharges were constructed using bin size of 0.34 radians.

Methodological considerations

No phenotypic marker is currently available for the exclusive identification of the preBötC. Here we used a combination of criteria to ascertain the location of injection site. We first located the preBötC by recording inspiration-related neuronal activity, starting at the caudal edge of the facial nucleus, along a series of descents made within a distance of $500 – 800$ μm behind the transverse sinus. In addition to the recording of inspiratory cells prior to tracer injection, post-hoc histology revealed that injection sites were located beneath the ambiguous nucleus at a distance of $600 – 900$ μm behind the caudal edge of the facial nucleus. In agreement with previous studies, axonal projections to the raphe nucleus, the para-hypoglossal region and the contralateral preBötC were also observed (Stornetta et al., 2003; Bouvier et al., 2010; Koizumi et al., 2013). Injection sites that did not fulfill all of these criteria were not considered in the present report.

Supplementary Material

Refer to Web version on PubMed Central for supplementary material.

Acknowledgments

References

Abbott SBG, Stornetta RL, Coates MB, Guyenet PG. Phox2b-expressing neurons of the parafacial region regulate breathing rate, inspiration, and expiration in conscious rats. J Neurosci. 2011; 31:16410–16422. [PubMed: 22072691]

Ashwell KW. The adult mouse facial nerve nucleus: morphology and musculotopic organization. J Anat. 1982; 135:531–538. [PubMed: 7153172]

Bouvier J, Thoby-Brisson M, Renier N, Dubreuil V, Ericson J, Champagnat J, Pierani A, Chédotal A, Fortin G. Hindbrain interneurons and axon guidance signaling critical for breathing. Nat Neurosci. 2010; 3:1066–1074. [PubMed: 20680010]

Deschênes M, Haidarliu S, Demers M, Moore J, Kleinfeld D, Ahissar E. Muscles involved in naris dilation and nose motion in rat. Anat Rec. 2015; 298:546–553.

Deschênes M, Kleinfeld D. Sniffing and whisking in rodents. Curr Opin Neurobiol. 2012; 22:243–250. [PubMed: 22177596]

Dorfl J. The musculature of the mystacial vibrissae of the white mouse. J Anat. 1982; 135:147–154. [PubMed: 7130049]

Feldman JL, Kam K. Facing the challenge of mammalian neural microcircuits: taking a few breaths may help. J Physiol. 2015; 593:3–23. [PubMed: 25556783]

Fortuna MG, West GH, Stornetta RL, Guyenet PG. Bötzinger expiratory-augmenting neurons and the parafacial respiratory group. J Neurosci. 2008; 28:2506–2515. [PubMed: 18322095]

Friauf E. Morphology of motoneurons in different subdivisions of the rat facial nucleus stained intracellularly with horseradish peroxidase. J Comp Neurol. 1986; 253:231–241. [PubMed: 3793991]

Furutani R, Izawa T, Sugita S. Distribution of facial motoneurons innervating the common facial muscles of the rabbit and rat. Okajimas Folia Anat Jpn. 2004; 81:101–108. [PubMed: 15747877]

Ganguly K, Kleinfeld D. Goal-directed whisking behavior increases phase-locking between vibrissa movement and electrical activity in primary sensory cortex in rat. PNAS. 2004; 101:12348–12353. [PubMed: 15297618]

Gao P, Hattox AM, Jones LM, Keller A, Zeigler HP. Whisker motor cortex ablation and whisker movement patterns. Somatosens Mot Res. 2003; 20:191–198. [PubMed: 14675958]

Gray PA, Janczewski WA, Mellen N, McCrimmon DR, Feldman JL. Normal breathing requires preBötzinger complex neurokinin-1 receptor-expressing neurons. Nat Neurosci. 2001; 9:927–930. [PubMed: 11528424]

Guyenet PG, Wang H. Pre-Bötzinger neurons with preinspiratory discharges "in vivo" express NK1 receptors in the rat. J Neurophysiol. 2001; 86:438–446. [PubMed: 11431523]

Haidarliu S, Golomb D, Kleinfeld D, Ahissar E. Dorsorostral snout muscles in the rat subserve coordinated movement for whisking and sniffing. Anat Rec. 2012; 295:1181–1191.

Haidarliu S, Kleinfeld D, Deschênes M, Ahissar E. The musculature that drives active touch by vibrissae and nose in mice. Anat Rec. 2015; 298:1347–1358.

Haidarliu S, Simony E, Golomb D, Ahissar E. Muscle architecture in the mystacial pad of the rat. Anat Rec. 2010; 293:1192–1206.

Herfst LJ, Brecht M. Whisker movements evoked by stimulation of single motor neurons in the facial nucleus of the rat. J Neurophysiol. 2008; 99:2821–2832. [PubMed: 18353915]

Hill DN, Bermejo R, Zeigler HP, Kleinfeld D. Biomechanics of the vibrissa motor plant in rat: rhythmic whisking consists of triphasic neuromuscular activity. J Neurosci. 2008; 28:3438–3455. [PubMed: 18367610]

Hinrichsen CF, Watson CD. The facial nucleus of the rat: representation of facial muscles revealed by retrograde transport of horseradish peroxidase. Anat Rec. 1984; 209:407–415. [PubMed: 6465545]

Klein BG, Rhoades RW. Representation of whisker follicle intrinsic musculature in the facial motor nucleus of the rat. J Comp Neurol. 1985; 232:55–69. [PubMed: 3973083]

Kleinfeld D, Deschênes M, Wang F, Moore JD. More than a rhythm of life: breathing as a binder of orofacial sensation. Nat Neurosci. 2014; 17:647–551. [PubMed: 24762718]

Koizumi H, Koshiya N, Chia JX, Cao F, Nugent J, Zhang R, Smith JC. Structural-functional properties of identified excitatory and inhibitory interneurons within pre-Bötzinger complex respiratory microcircuits. J Neurosci. 2013; 33:2994–3009. [PubMed: 23407957]

Komiyama M, Shibata H, Susuki T. Somatotopic representation of facial muscles within the facial nucleus of the mouse. A study using the retrograde horseradish peroxidase and cell degeneration techniques. Brain Behav Evol. 1984; 24:144–151. [PubMed: 6466963]

Mitchinson B, Martin CJ, Grant RA, Prescott TJ. Feedback control in active sensing: rat exploratory whisking is modulated by environmental contact. Proc R Soc Lond Biol Sci. 2007; 274:1035–1041.

Mitra PP, Pesaran B. Analysis of dynamic brain imaging data. Biophysical J. 1999; 76:691–708.

Moore JD, Deschênes M, Furuta T, Huber D, Smear MC, Demers M, Kleinfeld D. Hierarchy of orofacial rhythms revealed through whisking and breathing. Nature. 2013; 469:53–57.

Moore JD, Deschênes M, Kurnikova A, Kleinfeld D. Activation and measurement of free whisking in the lightly anesthetized rodent. Nat Prot. 2014; 9:1792–1802.

Nguyen Q-T, Wessel R, Kleinfeld D. Developmental regulation of active and passive membrane properties in rat vibrissa motoneurons. J Physiol. 2004; 556:203–219. [PubMed: 14766934]

Pagliardini S, Janczewski WA, Tan W, Dickson CT, Deisseroth K, Feldman JL. Active expiration induced by excitation of ventral medulla in adult anesthetized rats. J Neurosci. 2011; 31:2895–2905. [PubMed: 21414911]

Pinault D. A novel single-cell staining procedure performed in vivo under electrophysiological control: morpho-functional features of juxtacellularly labeled thalamic cells and other central neurons with biocytin or Neurobiotin. J Neurosci Meth. 1996; 65:113–136.

Ranade S, Hangya B, Kepecs A. Multiple modes of phase locking between sniffing and whisking during active exploration. J Neurosci. 2013; 33:8250–8256. [PubMed: 23658164]

Sachdev RHS, Berg RW, Chompney G, Kleinfeld D, Ebner FF. Unilateral vibrissa contact: Changes in amplitude but not the timing of vibrissa movement. Somato Mot Res. 2003; 20:162–169.

Shao XM, Feldman JL. Respiratory rhythm generation and synaptic inhibition of expiratory neurons in pre-Bötzinger complex: differential roles of glycinergic and GABAergic neural transmission. J Neurophysiol. 1997; 77:1853–1860. [PubMed: 9114241]

Sherrey JH, Megirian D. State dependence of upper airway respiratory motoneurons: Functions of the cricothyroid and nasolabial muscles of the unanesthetized rat. EEG Clin Neurophysiol. 1977; 43:218–228.

Sirotin YB, Costa ME, Laplagne DA. Rodent ultrasonic vocalizations are bound to active sniffing behavior. Front Behav Neurosci. 2014; 8:1–12. [PubMed: 24478648]

Sreenivasan V, Karmakar K, Rijli F, Petersen CH. Parallel pathways from motor and somatosensory cortex for controlling whisker movements in mice. Eur J Neurosci. 2015; 11:354–367. [PubMed: 25476605]

Stornetta RL, Rosin DL, Wang H, Sevigny CP, Weston MC, Guyenet PG. A group of glutamatergic interneurons expressing high levels of both neurokinin-1 receptors and somatostatin identifies the region of the pre-Bötzinger complex. J Comp Neurol. 2003; 455:499–512. [PubMed: 12508323]

Takatoh J, Nelson A, Zhou X, Bolton MM, Ehlers MD, Arenkiel BR, Mooney R, Wang F. New modules are added to vibrissal premotor circuitry with the emergence of exploratory whisking. Neuron. 2013; 77:346–360. [PubMed: 23352170]

Tan W, Pagliardini S, Yang P, Janczewski WA, Feldman JL. Projections of preBötzinger complex neurons in adult rats. J Comp Neurol. 2010; 518:1862–1278. [PubMed: 20235095]

Tan W, Janczewski WA, Yang P, Shao XM, Callaway EM, Feldman JL. Silencing preBötzinger complex somatostatin-expressing neurons induces persistent apnea in awake rat. Nat Neurosci. 2008; 11:538–540. [PubMed: 18391943]

Towal RB, Hartmann MJ. Right-left asymmetries in the whisking behavior of rats anticipate movements. J Neurosci. 2006; 26:8838–8846. [PubMed: 16928873]

Toyoda H, Ohno K, Yamada J, Ikeda M, Okabe A, Sato K, Hashimoto K, Fukuda A. Induction of NMDA and GABAA receptor-mediated Ca2+ oscillations with KCC2 mRNA downregulation in injured facial motoneurons. J Neurophysiol. 2003; 89:1353–1362. [PubMed: 12612004]

Wang H, Stornetta RL, Rosin DL, Guyenet PG. Neurokinin-1 receptor-immunoreactive neurons of the ventral respiratory group in the rat. J Comp Neurol. 2001; 434:128–146. [PubMed: 11331521]

Watson CR, Sakai S, Armstrong W. Organization of the facial nucleus in the rat. Brain Behav Evol. 1982; 20:19–28. [PubMed: 7104668]

Welker WI. Analysis of sniffing of the albino rat. Behaviour. 1964; 12:223–244.
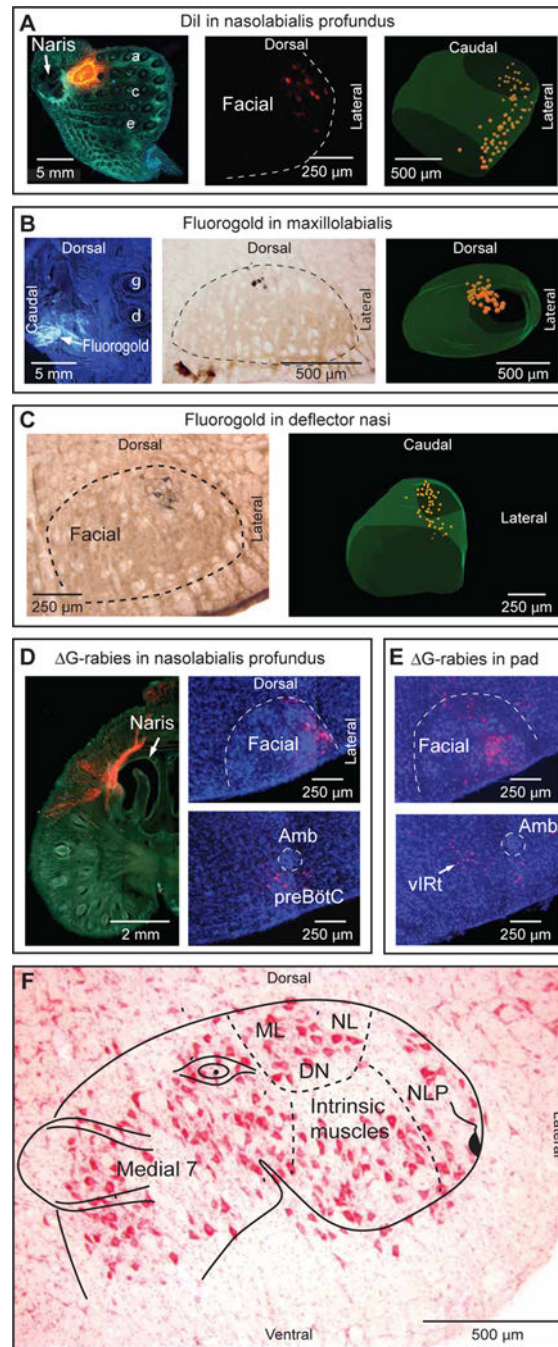
Figure 1. Muscle representation in the facial motor nucleus
(**A**) After insertion of a small pellet of Gelfoam saturated with DiI in the rat's snout, labeled motoneurons are found at the lateral edge of the facial nucleus. a,c,e, denote corresponding vibrissa rows. (**B**) Injection of Fluorogold in muscle maxillolabialis produces retrograde labeling in the dorsal sector of the facial nucleus. γ and δ denote corresponding vibrissae. (**C**) Injection of Fluorogold in muscle deflector nasi labels motoneurons in the dorsolateral sector of the facial nucleus. (**D**) ΔG-rabies injection in the snout labels motoneurons at the lateral edge of the facial nucleus, and premotor neurons in the preBötC. Amb, ambiguous

nucleus. **(E)** G-rabies injection into the mystacial pad labels motoneurons in the ventral lateral sector of the facial nucleus, and premotor neurons in vIRt. **(F)** Myotopic map of muscle representation on a Nissl-stained frontal section of the facial nucleus. The cartoon representation was adapted from ref 16. DN, muscle deflector nasi; ML, muscle maxillolabialis; NL, muscle nasolabialis; NLP, muscles nasolabialis profundus.
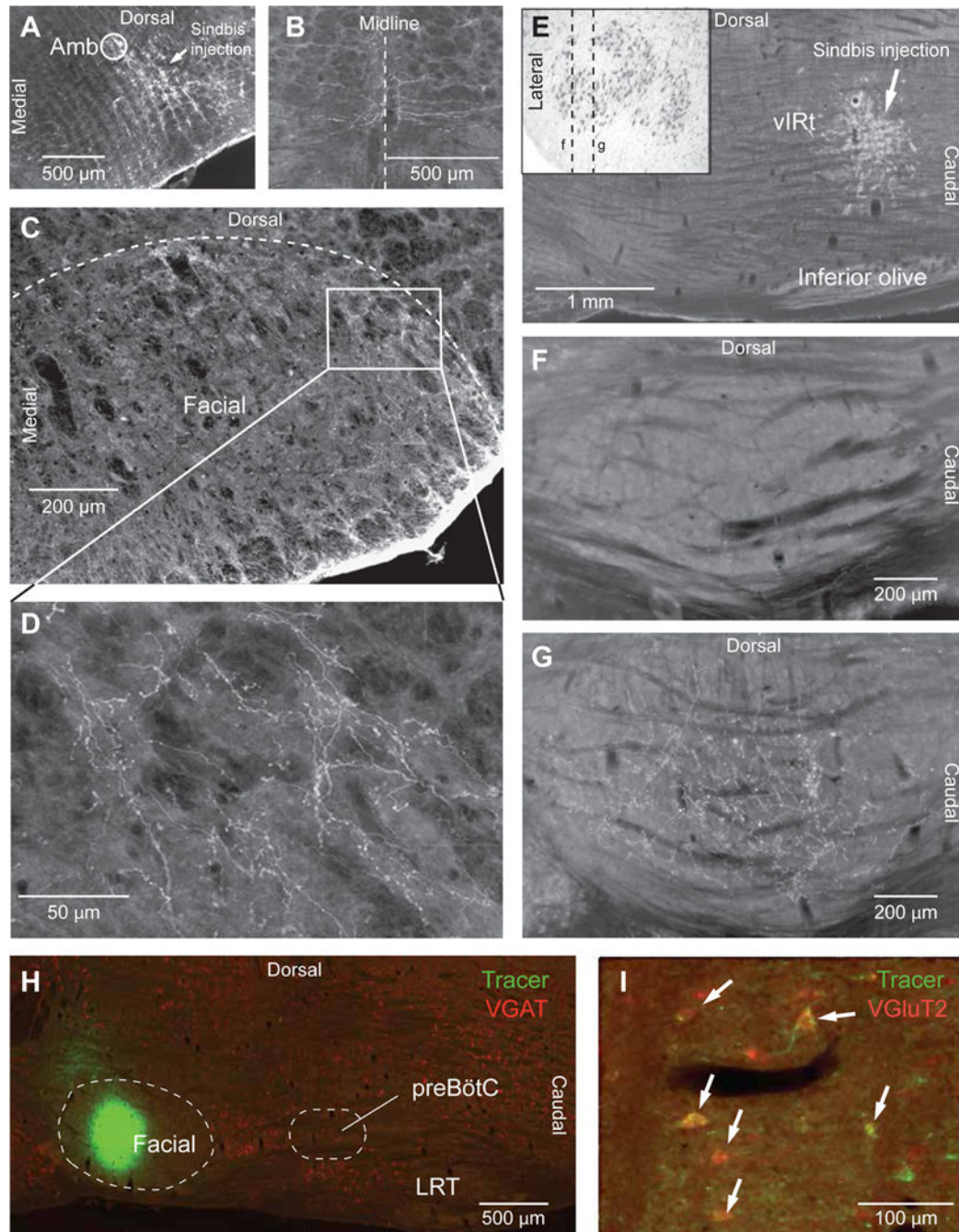
Figure 2. Differential projections of preBötC and vIRt to the facial nucleus
(**A–D**) Sindbis-GFP injection in preBötC labels commissural fibers (B), and axonal terminals in the lateral most sector of the facial nucleus (C). The framed area in C is enlarged in D. Frontal sections were stained for cytochrome oxidase, and colors were inverted to enhance contrast. (**E–G**) After Sindbis-GFP injection into vIRt, the lateral most sector of the facial nucleus is devoid of terminal labeling (F), whereas dense labeling is present in the ventral lateral sector of the nucleus (G). Sagittal sections in F and G correspond to section planes indicated by dashed lines in the Nissl-stained frontal section

shown in the insert (E). Sections were stained for cytochrome oxidase, and colors were inverted to enhance contrast. **(H–I)** Fluorogold was injected into the facial nucleus (H), and in situ hybridization was used to reveal the expression of the VGLUT2 and VGAT transcripts in labeled cells (I). Arrows indicate doubly labeled VGLUT2+ neurons. LRT, lateral reticular nucleus.
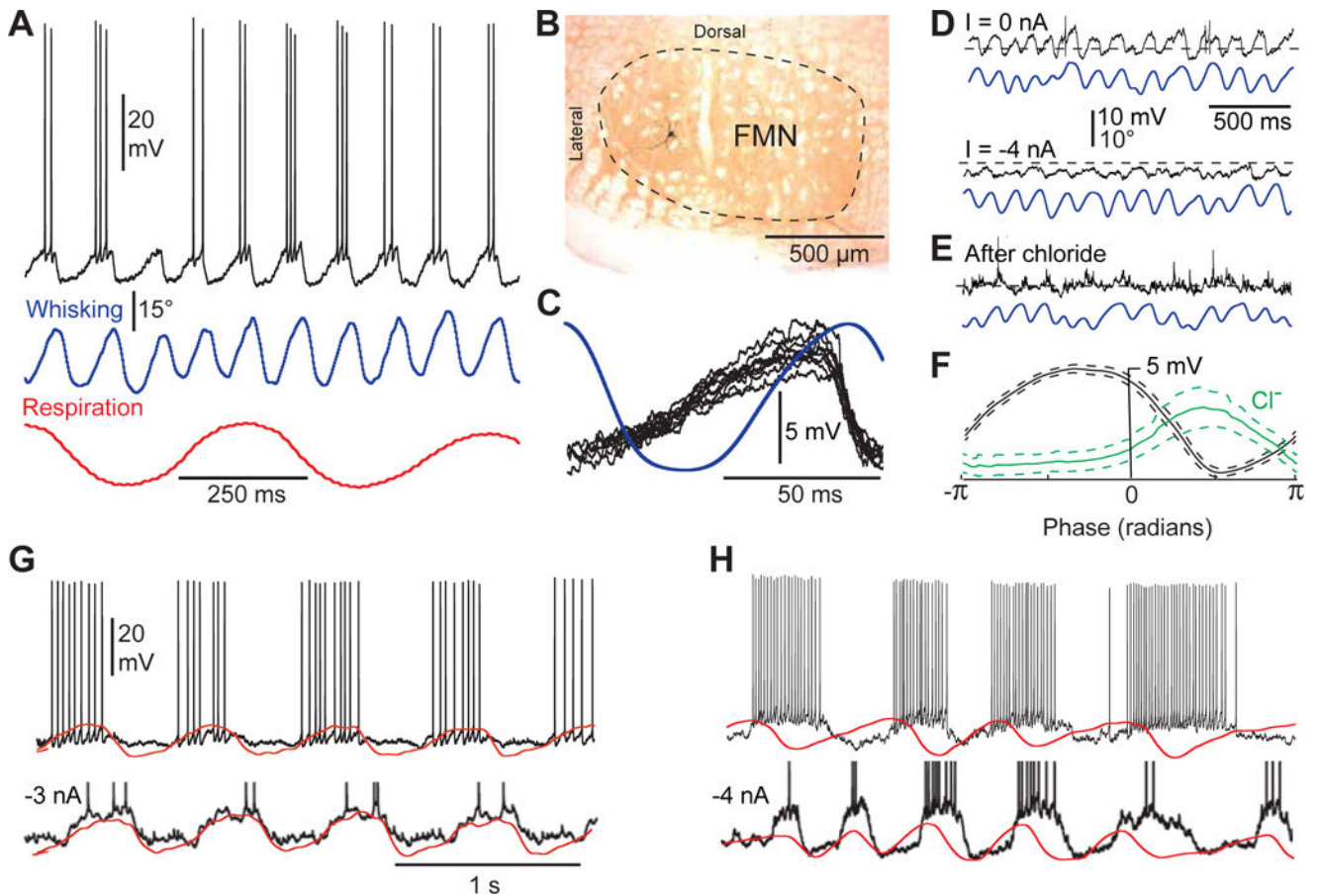
Figure 3. Oscillatory activity of facial motoneurons during KA-induced whisking
(A) Subthreshold oscillations and spike discharges are phase locked to vibrissa protraction in whisking motoneurons. In all figures vibrissa protraction and inspiration are up. **(B)** Motoneuron shown in A was labeled with Neurobiotin. **(C)** Ten superimposed traces of sawtooth-like subthreshold depolarizations associated with vibrissa protraction in another whisking motoneuron. Traces are aligned with respect to the peak of vibrissa protraction. The blue trace is the average of 10 whisks. Note the sharp repolarization just before the onset of vibrissa retraction. **(D)** The amplitude of subthreshold oscillations is depressed by hyperpolarizing current injection. **(E)** Chloride injection in the same motoneuron leads to reversal of the intracellular oscillation. **(F)** Plots of the phase of membrane potential oscillations before (black trace) and after chloride injection (green trace). Phase plots represent the average of 30 whisks, phase zero corresponding to the peak of protraction. Spikes were removed with a median filter (window, 30 ms) before averaging. Dashed lines indicate 95% confidence interval. **(G)** Membrane potential oscillations in inspiratory motoneurons increase in amplitude during hyperpolarizing current injection. Action potentials are cropped in the lower trace. **(H)** Membrane potential oscillations in expiratory motoneurons increase in amplitude during hyperpolarizing current injection. Action potentials are cropped in the lower trace. Scale bars in G apply in H.
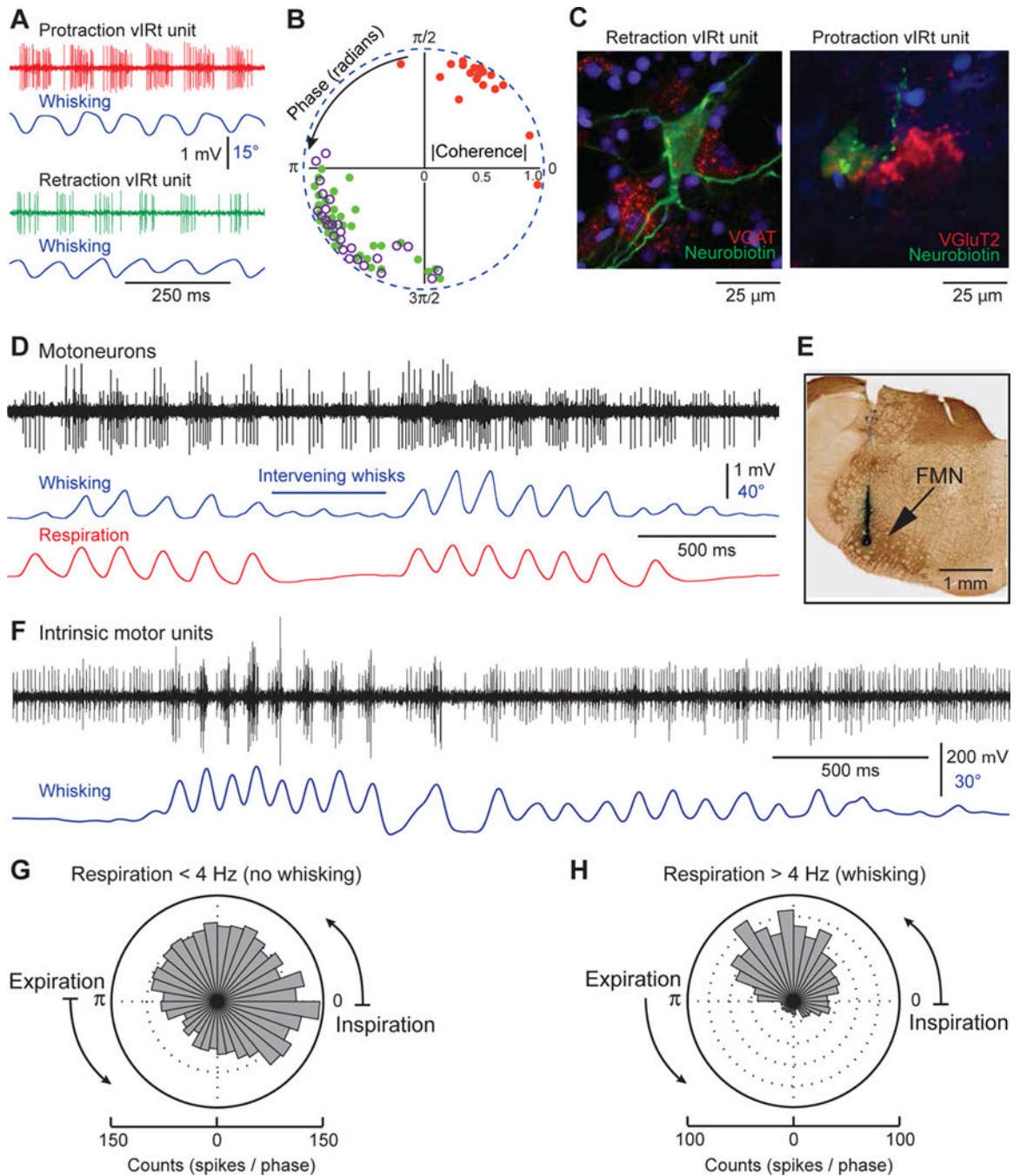
Figure 4. vIRt cells rhythmically inhibit vibrissa facial motoneurons
(**A**) During whisking induced by KA injection in the medulla, vIRt cells display antiphasic firing patterns. (**B**) Polar plot of the coherence between spiking activity and vibrissa motion at the peak frequency of whisking. Red and green dots represent protraction units and retraction units, respectively, which were recorded under ketamine/xylazine anesthesia. Purple circles represent vIRt units that were recorded under urethane anesthesia. Over 200 whisks per cell were used to compute phase angle and coherence. (**C**) Expression of VGAT and VGluT2 transcripts in individual vIRt cells labeled juxtacellularly with Neurobiotin. (**D**)

Firing of facial motoneurons during whisking in a head-restrained rat. Both cells discharge during vibrissa protraction, including whisks that are not associated with a breath (intervening whisks). The positive unit is recruited as whisk amplitude increases. **(E)** Labeling of the recording site by an iontophoretic deposit of Chicago sky blue. FMN, facial motor nucleus. **(F)** Motor units of the intrinsic vibrissa muscles are inhibited during vibrissa retraction. **(G–H)** Circular phase histograms of intrinsic motor unit discharges during basal respiration, and during sniffing associated with whisking. Histograms were built from 15 sequences containing both basal respiration and sniffing bouts in 3 rats (149 breaths and 120 sniffs).
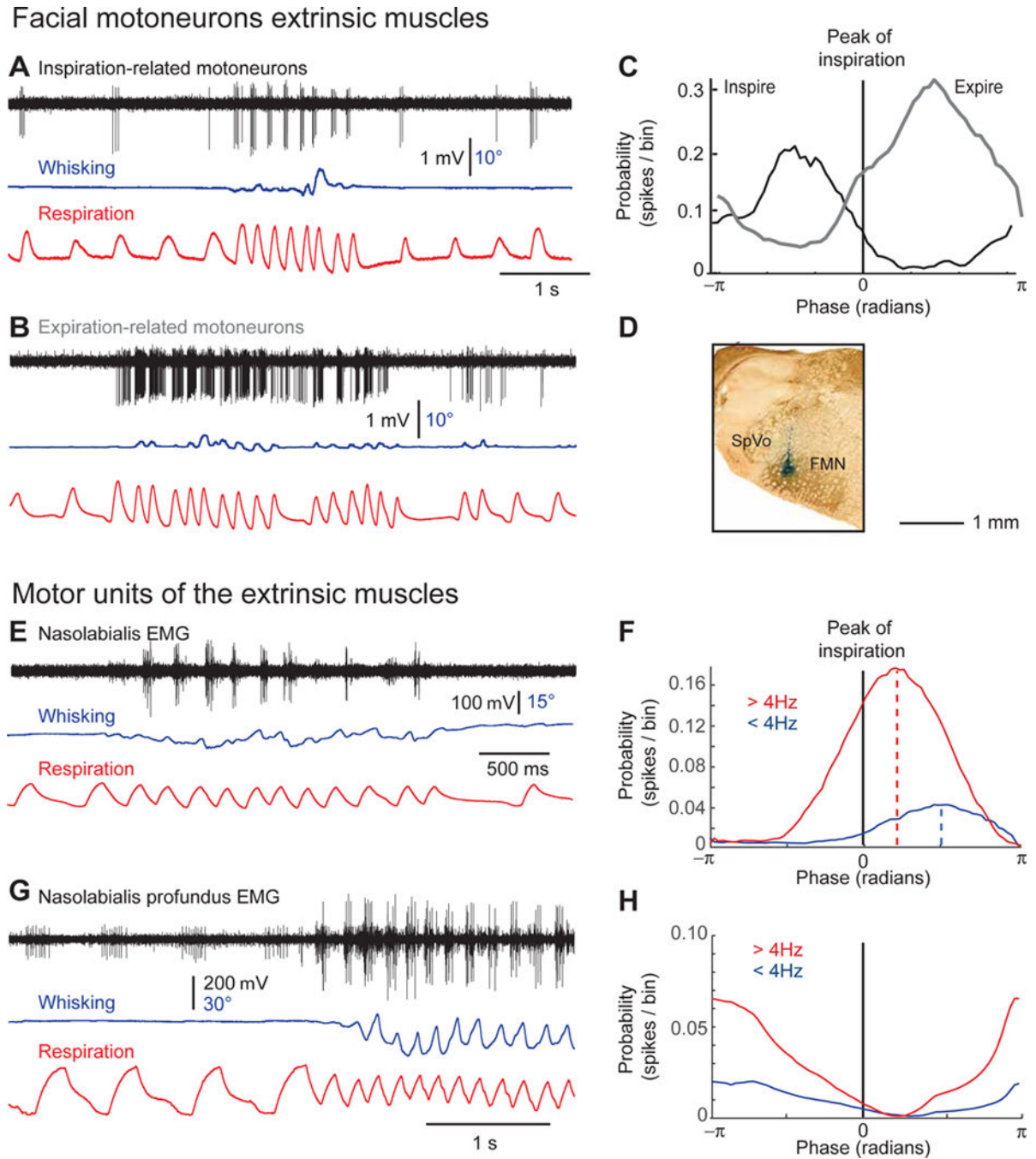
Facial motoneurons extrinsic muscles

A Inspiration-related motoneurons

Whisking

1 mV | 10°

Respiration

1 s

B Expiration-related motoneurons

1 mV | 10°

C

Peak of inspiration

Inspire — Expire

Probability (spikes / bin)

0.3
0.2
0.1
0

−π   0   π

Phase (radians)

D

SpVo
FMN

1 mm

Motor units of the extrinsic muscles

E Nasolabialis EMG

Whisking

100 mV | 15°

Respiration

500 ms

F

Peak of inspiration

> 4Hz
< 4Hz

Probability (spikes / bin)

0.16
0.12
0.08
0.04
0

−π   0   π

Phase (radians)

G Nasolabialis profundus EMG

Whisking

200 mV
30°

Respiration

1 s

H

> 4Hz
< 4Hz

Probability (spikes / bin)

0.10

0.05

0

−π   0   π

Phase (radians)

Figure 5. Conditional activation of facial motoneurons during sniffing in head-restrained rats
(A,B) Discharges of respiratory motoneurons during basal respiration and sniffing. Note that in these two examples sniffing occurs without significant whisking. **(C)** Phase plots of motoneuronal discharges across a population of five inspiratory motoneurons (solid line; 572 inspirations), and 7 expiratory motoneurons (dashed line; 974 expirations). **(D)** The recording site of the neuron shown in (B) was labeled with a deposit of Chicago sky blue. **(E)** EMG recording of nasolabialis motor units during basal respiration and sniffing. Note that muscle nasolabialis preferentially contracts in phase with expiration during sniffing. **(F)**

Phase plots of muscle nasolabialis motor units activity during basal respiration (< 4Hz; 1180 breaths) and sniffing (> 4Hz; 1725 sniffs). Note the stronger modulation during sniffing, and the phase shift of activity between basal respiration and sniffing. **(G)** EMG recording of nasolabialis profundus motor units during basal respiration and sniffing. Note that the small unit is active during both basal respiration and sniffing, while the large unit is active during sniffing. **(H)** Phase plots of muscle nasolabialis motor units activity during basal respiration (< 4Hz; 668 breaths) and sniffing (> 4Hz; 756 sniffs). Note the stronger modulation during the inspiratory phase of sniffing.
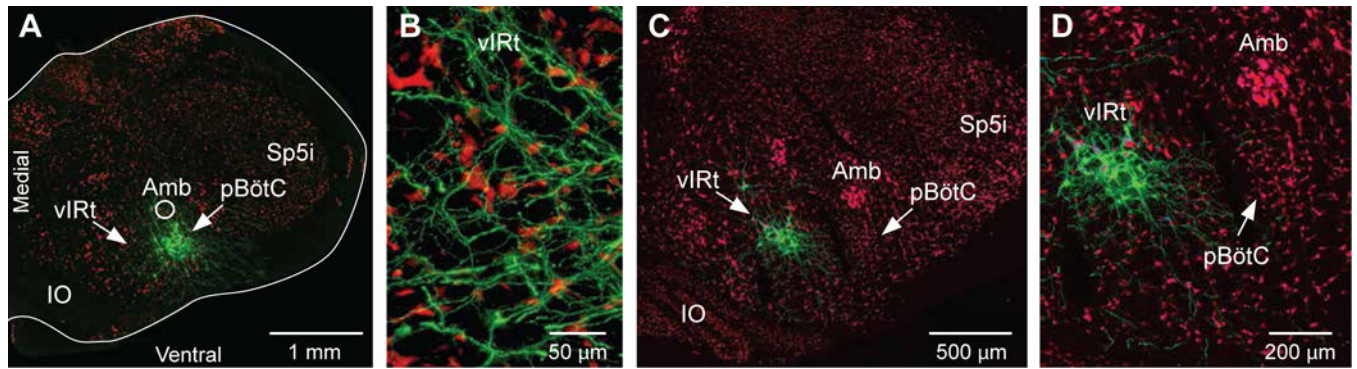
Figure 6. Unidirectional connections between preBötC and vIRt
(A) Sindbis-GFP injection in preBötC produces anterograde labeling in vIRt. **(B–C)** In contrast, Sindbis-GFP injection into vIRt (C) does not label terminals in preBötC. **(D)** Sections were immunostained with an anti-NeuN antibody. Amb, ambiguous nucleus; IO, inferior olive; Sp5i, interpolaris division of the spinal trigeminal nucleus.
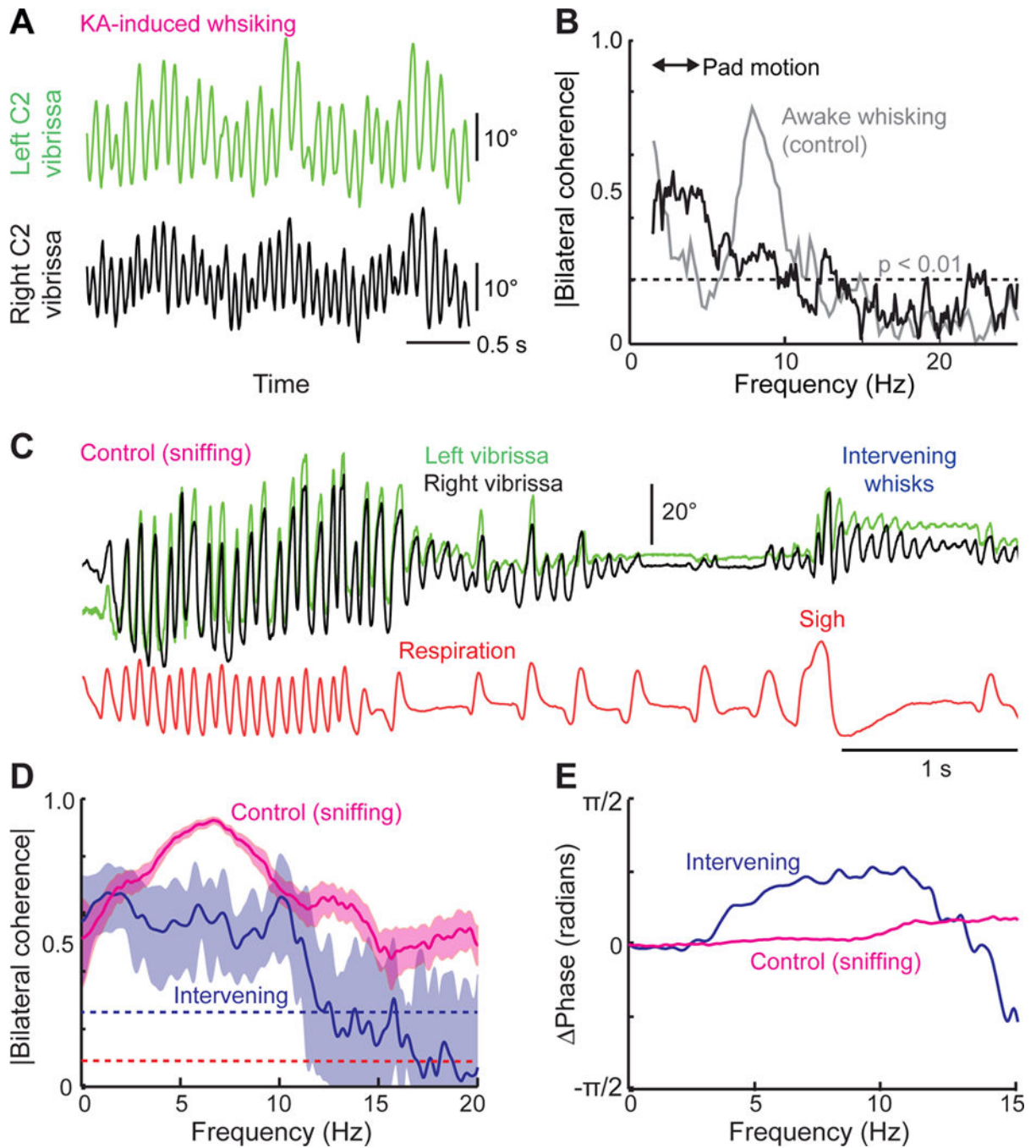
Figure 7. The left and right whisking oscillators are independent from one another
(A) Bilateral kainic acid injection produces independent vibrissa movements on the left and right sides of the face. **(B)** Spectral coherence (black trace) between the movements of each of the vibrissae in (A). The two signals show low coherence in the band of whisking frequencies relative to control data for bilateral active whisking in alert animals (gray trace). **(C)** Representative traces of whisking and respiration used to compute average bilateral coherence between sniff-related and intervening whisks in three head-restrained rats. **(D)** Average coherence between left and right intervening whisks is lower than that of sniff-

related whisks. Light blue and red areas represent 95% confidence interval. **(E)** Whisks on the left and right sides of the face display virtually no phase difference during sniff-related whisks (red line), whereas intervening whisks display a clear phase shift (blue line).
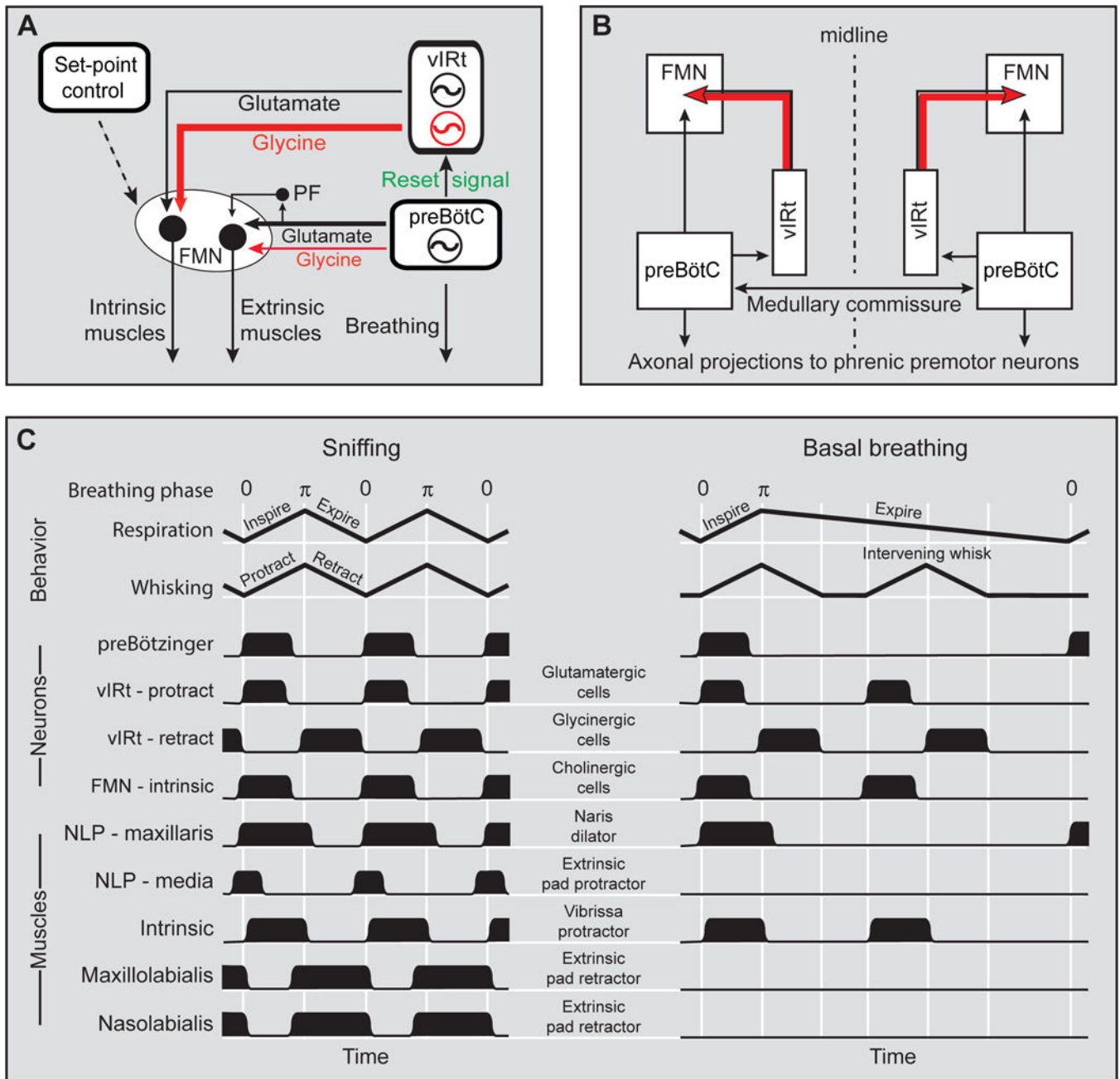
Figure 8. Model of the medullary circuitry that generates whisking in coordination with breathing

(A) The core of the whisking CRG consists of glycinergic/GABAergic cells that inhibit motoneurons that innervate the intrinsic vibrissa muscles. The drive for vibrissa protraction arises from a smaller population of glutamatergic vIRt cells, and from other excitatory and modulatory inputs that control the set-point of whisking. The extrinsic muscles are driven by the respiratory CRG, with a potential contribution from parafacial neurons (PF) that receive input from the preBötC. **(B)** The reset of whisking by breathing is mediated by unidirectional connections from preBötC to vIRT, and commissural fibers that connect the left and right preBötCs ensure bilateral synchronization of whisking. **(C)** Idealized time-

ordered patterns of behavioral, neuronal and muscular activities associated with the different phases of the respiratory and whisking rhythms. Note that the extrinsic pad retractor and protractor muscles may activate during basal respiration when the amplitude of respiration increases.